

1 **Detection of novel *Plasmodium falciparum* haplotypes under treatment pressure in pediatric**
2 **severe malaria**

3 Balotin Fogang¹, Emilie Guillochon², Claire Kamaliddin^{2&}, Gino Agbota^{2,3}, Sem Ezinmegnon^{2,3},
4 Maroufou Jules Alao⁴, Philippe Deloron², Gwladys Bertin², Antoine Claessens^{1*}

5 1 LPHI, CNRS, INSERM, University of Montpellier, Montpellier, France

6 2 Université Paris Cité, MERIT, IRD, Paris, France

7 3 Institut de Recherche Clinique du Bénin (IRCB), Abomey-Calavi, Benin

8 4 Paediatric Department, Mother and Child University and Hospital Center (CHU-MEL), Cotonou,
9 Benin

10 & Current affiliation: Cumming School of Medicine, The University of Calgary, Calgary, Alberta,
11 Canada

12 *Correspondence antoine.claessens@umontpellier.fr

13 **Keywords.** *Plasmodium falciparum*, genetic complexity, parasite clearance, severe malaria

14 **Abstract**

15 **Background.** In Africa, the clearance time for *P. falciparum* severe malaria varies significantly,
16 likely due to the complexity of *P. falciparum* infections and the sequestration phenomenon
17 exhibited by this parasite. This study aims to evaluate different methods to study intra-host
18 dynamics of polygenomic infections during parasite clearance under antimalarial treatment.
19 Additionally, it seeks to determine the association between parasite clearance rate following
20 artesunate or quinine treatment and the genetic complexity of *P. falciparum* in Beninese children
21 with severe malaria.

22 **Methods.** Sixty-five *P. falciparum* severe malaria individuals diagnosed by microscopy and treated
23 with artesunate or quinine were sampled every 8 hours for 24 hours. Using whole genome
24 sequencing (WGS) data, we estimated the multiplicity of infection (MOI) with three algorithms
25 (*Fws*, THE REAL McCOIL, and RoH). We then characterized the *P. falciparum* genetic
26 complexity in WGS-identified polyclonal infections using amplicon sequencing (AmpSeq) on DNA
27 extracted from plasma and from the red blood cells pellet.

28 **Results.** AmpSeq demonstrated greater sensitivity in detecting multiple genomes within isolates
29 compared to WGS methods. The MOI from AmpSeq was significantly higher in RBC pellets
30 compared to plasma (2.4 vs 1.8 distinct microhaplotypes per isolate). However, at parasitaemia over
31 1000 parasites/uL, the same MOI was detected in both plasma and pellet samples in 85.4% of the
32 isolates. We observed a high variability in parasite clearance rate among participants, but it was not
33 associated with parasite MOI at diagnostic. Interestingly, in 60.9% of participants, previously
34 undetected microhaplotypes appeared in circulation 16 hours after treatment initiation.

35 **Conclusion.** These findings demonstrate that combining different haplotyping techniques
36 effectively determines parasite genetic complexity. Additionally, plasma can be effectively used for
37 parasite genotyping at sufficient parasitaemia levels. The parasite clearance rate of severe malaria is
38 independent of parasite MOI. However, genotyping a single blood sample upon hospital admission
39 does not capture the full spectrum of parasite genotypes present in the infection.

40 **Keywords.** *Plasmodium falciparum*, genetic complexity, parasite clearance, severe malaria

41 **Introduction**

42 *Plasmodium falciparum* is the predominant malaria species and a major contributor to child
43 mortality in Africa. Many children infected with *P. falciparum* succumb to the disease before even
44 reaching a hospital or clinic. Among those who are admitted with severe malaria and receive
45 parenteral antimalarial treatment, approximately 5% do not survive, highlighting the urgent need for
46 effective interventions [1]. Since 2011, the World Health Organisation (WHO) has recommended
47 intravenous artesunate as the first-line antimalarial treatment for severe malaria [2], citing its
48 potential to reduce severe malaria mortality rates by 22.5% compared to quinine [3]. Nevertheless,
49 in cases where artesunate is unavailable, alternative severe malaria treatment such as intramuscular
50 artemether or intravenous quinine are recommended [2].

51 Despite the widespread recommendation of Artemisinin-based Combination Therapies (ACTs) as
52 the frontline treatment for malaria, reports of *P. falciparum* resistance to ACTs have risen in Asia
53 [4, 5] and more recently in Africa [6, 7]. Indeed, artemisinin resistance is characterized by the slow
54 clearance of parasites *in vivo*, which is a result of reduced drug susceptibility in ring-stage parasites
55 driven by mutations in the *P. falciparum Kelch13* gene [8]. Since the introduction of artemisinin-
56 based combination therapy (ACT) in 2005, no Pfk₁₃ mutation associated with artemisinin
57 resistance has been identified in Benin [9, 10].

58 Although the *PfKelch13* polymorphisms are the strongest predictor of *in vivo* parasite clearance
59 time under treatment with artesunate, this time can be affected by other factors such as the age of
60 the host, host-acquired immunity, initial parasitemia levels, and the developmental stages of
61 parasite [11–13]. Although controversial, studies have shown a link between the genetic complexity
62 of *P. falciparum* and delayed parasite clearance in Africa. Indeed, children infected with multiple
63 strains had nearly a 3-fold increase in treatment failure compared to their age mates infected with a
64 single strain [14]. However, low multiplicity of infection (MOI) at baseline were associated with

65 detectable parasitaemia at 72h post-ACT treatment [15]. The association between antimalarial
66 parasite clearance rate and parasite genetic complexity in individuals with severe malaria (SM)
67 remains to be explored.

68 In SM, the delay in parasite clearance could also be attributed to the significant sequestration of
69 mature *P. falciparum* parasitized erythrocytes within the tissue capillaries. Mathematical modelling
70 using plasma histidine-rich protein 2 (PfHRP2) levels and parasitaemia have indicated that the
71 number of sequestered parasites is substantially higher than what is detected in the peripheral blood
72 [16–18]. Because the circulating parasitaemia is highly dependent on the parasite developmental
73 stage, the amount of *Plasmodium* DNA in plasma is actually more accurate than parasitemia for
74 diagnostic differentiating severe from uncomplicated malaria [19]. Other studies have also
75 demonstrated that plasma can be used to detect and quantify the *Plasmodium* DNA by PCR [20,
76 21]. However, whether genomic DNA (gDNA) extracted from plasma could be used as material to
77 reliably estimate the MOI is not known. Although the plasma may contain less parasite DNA than
78 within RBCs, it is unaffected by sequestration and could theoretically contain parasite DNA
79 released from prior schizont ruptures of all the parasite genotypes present within an individual.
80 However, there is currently no evidence regarding the sensitivity of *Plasmodium* genotyping when
81 using plasma samples as the DNA source.

82 Various sequencing approaches have recently been used to assess the complexity of *P. falciparum*,
83 quantified as the number of parasite genotypes within an isolate [22]. These methods include
84 whole-genome sequencing (WGS)-based techniques using diverse metrics such as *F_{ws}* [23], THE
85 REAL McCOIL [24], and Runs of Homozygosity (RoH) [25], which elucidate intra-host parasite
86 diversity by analysing genome-wide variations across multiple loci. *F_{ws}* is a metric characterizing
87 within-host diversity and its relationship to population-level diversity, with theoretical values
88 ranging from 0 to 1. The RoH indicates genetic relatedness between 2 or more genotypes within an
89 isolate by identifying long blocks of haplotypes that have been inherited from the same parent. The
90 REAL McCOIL is a statistical approach that uses data from all infections to simultaneously

91 estimate allelic frequency and the number of distinct genotypes s in an isolate. Amplicon
92 sequencing (AmpSeq), a technique targeting highly polymorphic loci, has emerged as a novel tool
93 capable of detecting minority microhaplotypes with within-sample frequencies as low as 0.1% [26].
94 Indeed, the strength of sequencing targeted non-repetitive regions that harbour extensive single
95 nucleotide polymorphisms (SNPs) lies in the fact that all SNPs within an amplicon are linked by a
96 single sequence read, enabling direct microhaplotype identification [26]. Therefore, this study aims
97 to evaluate the association between parasite clearance rate and multiplicity of infection in Beninese
98 children undergoing treatment for severe malaria, using a variety of sequencing methods and
99 biological materials.

100 **Methods**

101 **Study design**

102 Ethical clearance was obtained from “Comité d’Ethique de la Recherche CER_ISBA Benin”
103 (clearance n°90, 06/06/2016 and clearance n°38, 16/05/2014). During the high malaria transmission
104 season in Southern Benin, children under the age of six diagnosed with severe malaria infection at
105 the “Centre Hospitalier et Universitaire de la Mère et de l’Enfant-Lagune (CHU-MEL) de
106 Cotonou ” were enrolled in the study in both 2014 and 2016, as described in Kamaliddin 2019 [27].
107 Prior to their participation, written informed consent from parents or guardians was obtained.
108 Malaria infection was diagnosed in febrile patients by detecting *P. falciparum* on a Giemsa-stained
109 thick blood smear. Parasite density was estimated by counting the number of parasites per at least
110 200 white blood cells (WBC) and assuming a standard total blood WBC count of 8000 WBC/ μ L.
111 Diagnosis and classification of severe malaria were carried out in accordance with WHO guidelines
112 for the management of severe malaria [2]. In brief, cerebral malaria (CM) was characterised by
113 impaired consciousness, indicated by a Blantyre score < 3 , after excluding other causes of coma.
114 Severe anaemia (SMA) was identified by a haemoglobin level < 5 g/dL or a haematocrit level $<$

115 15%. Severe non-cerebral malaria (SNCM) was defined by the features of severe malaria excluding
116 CM involvement. Furthermore, clinical appreciation was at the discretion of the admitting
117 physician.

118 Approximately 5 mL of blood were collected from all participants using EDTA-coated tubes before
119 the administration of quinine (in 2014) or artesunate (in 2016) therapy (H0). Subsequently, three
120 additional blood samples were taken at +8 hours (H8), +16 hours (H16), and +24 hours (H24) post-
121 treatment initiation to capture parasite dynamics.

122 **DNA extraction**

123 Plasma was separated from total blood cells by centrifugation at 1500 rpm for 5 min and
124 immediately stored at -20°C . Red blood cell (RBC) pellet was obtained by depleting white blood
125 cells using a gradient-based separation technique Ficoll (GE Healthcare Life Science). *P.*
126 *falciparum* genomic DNA (gDNA) was extracted from both 200 μL of red blood cell (RBC) pellets
127 and 200 μL of plasma using the DNEasy Blood kit (QIAGEN) according to the manufacturer's
128 instructions.

129 **Complexity of infection using whole genome sequencing (WGS) data**

130 WGS was performed by the Malaria Genomic Epidemiology Network (MalariaGEN) and the
131 samples are part of the *Plasmodium falciparum* Community Project accessible at
132 <https://www.malariagen.net/project/p-falciparum-community-project/>. The raw reads are available
133 on the ENA server under the accession numbers specified in the Supplementary Table 1. Variant
134 Calling Files (VCF) was generated by MalariaGEN as previously described [28]. Briefly, reads
135 were mapped to *P. falciparum* 3D7 v3 reference genome using bwa mem, and the resulting BAM
136 files were subjected to cleaning using Picard tools and GATK. SNPs and indels were called using
137 GATK HaplotypeCaller, with only the core genome considered for analysis.

138 For downstream analysis bcftools v1.13 [29] and bedtools v2.30 [30] were used for file
139 manipulation. Samples with at least 50% coverage of the genome at 5x were considered. Fraction of
140 within-sample (F_{ws}) metrics were computed using the moimix R package, as previously described
141 (<https://github.com/bahlolab/moimix>). An F_{ws} value < 0.95 was indicative of a polyclonal
142 infection. THE REAL McCOIL categorical method was used to estimate the complexity of the
143 infection (MOI) as described by Chang et al. [24] ([https://github.com/Greenhouse-](https://github.com/Greenhouse-Lab/THEREALMcCOIL)
144 [Lab/THEREALMcCOIL](https://github.com/Greenhouse-Lab/THEREALMcCOIL)). Long runs of homozygosity (RoH) and the analysis of heterozygosity in
145 mixed samples were carried out using a custom Python script based on Pearson et al. [25].

146 **DNA preparation and amplicon sequencing**

147 Three AmpSeq markers, including the genes for conserved plasmodium membrane protein (*cpmp*,
148 PF3D7_0104100), conserved plasmodium protein (*cgp*, PF3D7_1475800) and apical membrane
149 antigen (*ama1-D3*, PF3D7_1133400) were amplified using nested-PCR, as described in [31].
150 Briefly, primary PCRs were conducted in multiplex for *cpmp/ama1-D3* and monoplex for *cgp*.
151 Nested PCRs were subsequently performed individually for each marker. All amplifications were
152 carried out using the KAPA HiFi Hot Start Ready Mix (Roche) on an Eppendorf Mastercycler
153 Nexus thermocycler. The quality and quantity of nested-PCR products were assessed through gel
154 electrophoresis. Following this, nested-PCR products from each sample were combined in the
155 following proportions: 11 μ L of *cpmp*, 8 μ L of *cgp*, and 4 μ L of *ama1-D3*, for a total of 25 μ L. PCR
156 primers and amplification conditions are shown in the Supplementary Table 2.

157 Libraries preparations and amplicon sequencing were performed by the Genseq platform of the
158 Labex CeMEB (Montpellier). Merged PCR products were purified, sequencing adapters and
159 multiplexing indices were linked by PCR. Indexed products were purified, pooled and quality was
160 verified by electrophoresis using The Fragment Analyzer system (Agilent Biotechnologies). PCR
161 products resulting from RBC pellet or plasma gDNA were separated in two different plates, to
162 prevent the impact of the difference in DNA concentration on the sequencing quality. Finally,

163 amplicon libraries were sequenced on an Illumina MiSeq system in paired-end mode (2 x 300
164 cycles, 300 bp). The raw AmpSeq reads are available on the Zenedo
165 (<https://zenodo.org/records/13224728>), with corresponding individual accession numbers provided
166 in Supplementary Table 3.

167 Markers haplotypes were reconstructed using HaplotypR R package [26], accessible at
168 <https://github.com/lerch-a/HaplotypR>. Briefly, the quality of raw reads data was assessed using
169 FastQC. Reads corresponding to each marker were demultiplexed based on primers sequences, with
170 subsequent truncation of primers. Reads were trimmed following sequence quality and then fused.
171 SNPs and microhaplotypes were called with default parameters, requiring a minimum coverage of 3
172 reads per microhaplotype, at least 25 reads coverage per sample, and a within-host microhaplotype
173 frequency $\geq 0.1\%$. Microhaplotype sequences that differ by less than two SNPs were deemed
174 identical. The relative frequency of each microhaplotype in an isolate was calculated by dividing
175 the number of reads for each microhaplotype by the total number of reads for that isolate. For
176 downstream analysis, marker showing the highest number of microhaplotypes in an individual was
177 retained. The same marker was chosen for the four time points in an individual. The raw data for
178 AmpSeq are presented in Supplementary Table 3.

179 **Statistical analysis**

180 All statistical analyses were performed using R software version 4.3.2 [32]. Median comparisons of
181 two quantitative variables were conducted using the Mann–Whitney test, while mean comparisons
182 were assessed using the unpaired t-test. The correlation between two quantitative variables was
183 assessed using the Spearman correlation test. For categorical variables, proportions were analysed
184 using the Chi-squared test. We used linear interpolation to estimate the time required for a 50%
185 reduction in parasitaemia, referred as the extrapolated parasite clearance half-life ($PC_{50\%}$). The
186 clearance curve for each microhaplotype (parasite genotype detected by AmpSeq) was calculated by
187 multiplying the parasitaemia at each time point by the relative frequency of each microhaplotype.

188 Shannon entropy was used to characterize the complexity of microhaplotypes within an isolate
189 obtained from AmpSeq.

190 Results

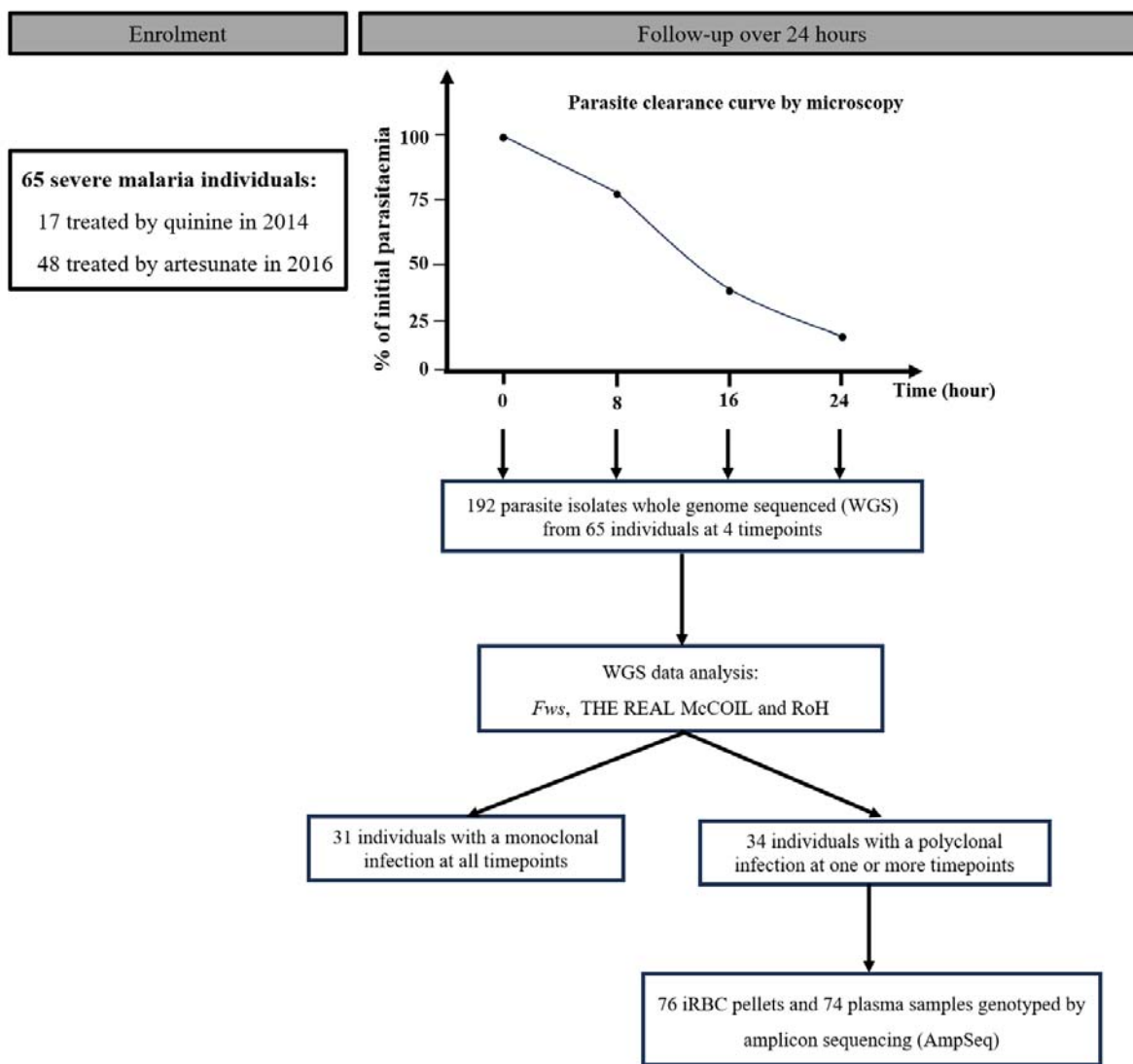
191 Characteristics of the study population

192 During the years 2014 and 2016, a total of 65 children aged 0 to 5 years old suffering from severe
193 malaria and admitted at CHU-MEL in Benin were recruited. Of these participants, 17 received
194 quinine in 2014, while 48 received artesunate in 2016 (Figure 1). These individuals were classified
195 as 26 cerebral malaria (CM), 16 severe non-cerebral malaria (SNCM) and 23 severe malaria
196 anaemia (SMA) (Supplementary Table 1). The median age and sex ratios of participants were
197 comparable between quinine and artemisinin treated groups. However, the geometric mean
198 parasitaemia in 2014 was significantly higher than in 2016 ($p < 0.0001$). The demographic and
199 parasitological characteristics of the participants at enrolment are provided in Table 1. Blood
200 samples were also collected on arrival at hospital and every 8 hours for 24 hours (Figure 1).

201 Table 1. Demographic and clinical background of the study participants

Characteristics	Artesunate	Quinine	p-value
Number of participants (N= 65)	48	17	
Sex ratio (M/F)	1.9 (27/14) NA= 7	1.3 (9/7) NA= 1	0.5506
Median age, months (range)	30 (5-60) NA= 5	36 (9-59)	0.2144
Geometric mean parasitaemia/ μ L (range)	66595 (405-2153565)	1317219 (15375-3200000)	< 0.0001

202



203

204 **Figure 1. Study flow diagram.** Sixty-five severe malaria patients were sampled at the start of
205 treatment and every 8 hours for 24 hours afterwards. Out of 230 isolates submitted for whole
206 genome sequencing, 192 yielded high-quality genomes. The multiplicity of infection (MOI) was
207 determined from parasite whole genome sequences. From 34 individuals with at least one
208 polyclonal timepoint, amplicon sequencing (AmpSeq) was performed on plasma and red blood cell
209 pellet samples. A total of 76 RBC pellet isolates and 74 plasma gDNA isolates from 23 individuals
210 were successfully genotyped.

211 **Determining the Multiplicity of Infection (MOI) based on Whole Genome Sequencing (WGS)**

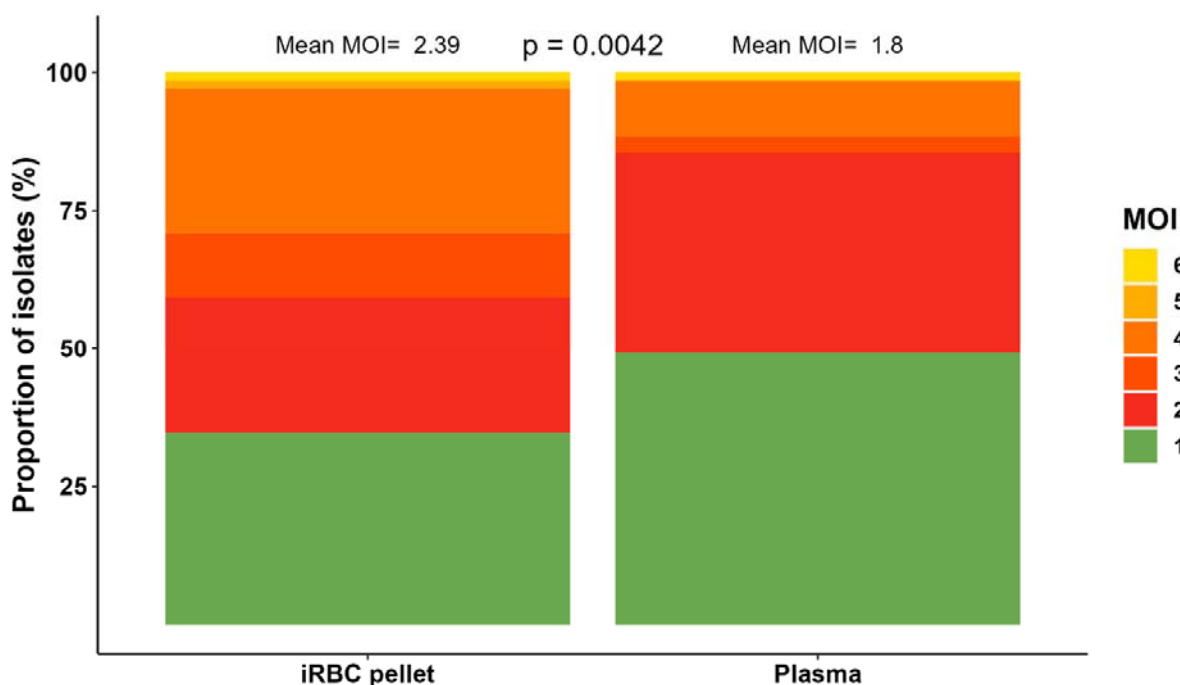
212 We first aimed to characterise the MOI using whole genome sequencing. A total of 230 RBC pellet
213 samples at each timepoint were whole genome sequenced, resulting in 192 good-quality genomes
214 (Figure 1 and Supplementary Table 1). To assess the MOI from these genomes, three algorithms
215 were tested: F_{WS} , THE REAL McCOIL and Runs of Homozygosity (RoH). All three algorithms
216 showed robust correlation (Appendix 1). From here onwards any genome with $F_{WS} > 0.95$ was
217 considered monoclonal.

218 **Determining the MOI based on AmpSeq using gDNA from RBC pellets and plasma**

219 We used the amplicon sequencing approach (AmpSeq) to assess MOI from paired RBC pellets and
220 plasma samples obtained from the same individuals. The rationale was that the RBC pellet
221 represents circulating parasites at a certain timepoint, while plasma could contain parasite DNA
222 from previous schizont ruptures that is independent of sequestration. As described in the methods
223 section, three markers were used (*cpmp*, *cpp*, *ama1*) and the marker showing the highest number of
224 microhaplotypes in an individual was retained (*cpmp*, *cpp* and *ama1* in 34.8%, 34.8% and 30.4% of
225 individuals, respectively, Supplementary Table 3). AmpSeq was successfully performed at each
226 timepoint sample from 23 individuals with a polyclonal infection, as determined by WGS methods.
227 69 isolates were successfully genotyped in both RBC pellets and plasma gDNA, 7 were genotyped
228 in RBC pellets gDNA only and 5 in plasma gDNA only (Supplementary Table 1).

229 In terms of sequence diversity, a total of 65 unique microhaplotypes were detected across all
230 isolates. Among these, 98.5% (64) were identified in pellets, while 70.8% (46) were found in
231 plasma. Furthermore, 19 microhaplotypes (29.2%) were exclusively present in pellets, while only
232 one microhaplotype was only found in plasma. The mean MOI per isolate was significantly higher
233 in RBC pellets compared to plasma (2.4 and 1.8 for pellets and plasma respectively, $p = 0.0042$)
234 (Figure 2). Among isolates from the same individual, 66.7% (46/69) exhibited an identical number
235 of genotypes detected when using gDNA from both RBC pellets and plasma. Furthermore, at

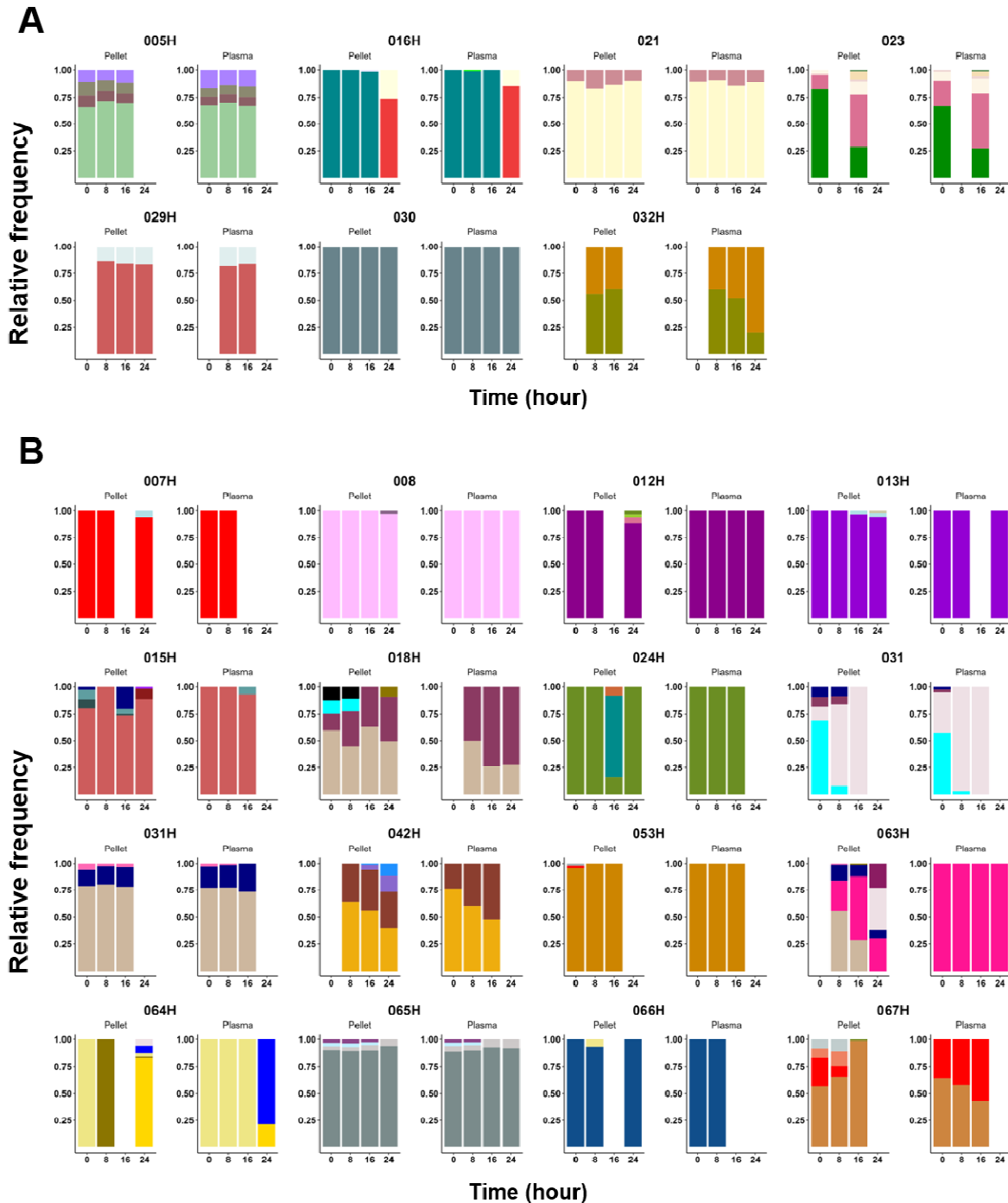
236 parasitaemia over 1000 parasites/uL, the same MOI was detected in both plasma and pellet samples
237 in 85.4% of the isolates (Supplementary Figure 1). This indicates the influence of parasite load on
238 the sensitivity of AmpSeq when using plasma as the source of DNA. However, these data also show
239 that plasma can be effectively used for parasite genotyping at relatively high parasitaemia levels.
240 By visualizing the evolution of clonality at each time point (0h, 8h, 16h and 24h) during the 24h
241 after treatment initiation (Figure 3), 7 infections showed the same MOI profile from RBC pellet and
242 plasma over time (Figure 3A), while in 16 infections more microhaplotypes were detected in RBC
243 pellet than in plasma (Figure 3B). Taken together, AmpSeq using gDNA from RBC pellets is more
244 sensitive compared to AmpSeq using gDNA from plasma at low range parasitaemia. From here
245 onwards, the AmpSeq MOI was defined as the number of microhaplotypes detected with gDNA
246 from RBC pellets.
247



248

249 **Figure 2.** Comparison of the multiplicity of the infection determined using AmpSeq with gDNA
250 from paired RBC pellet and plasma samples. The MOI per isolate, indicated as a colour scale, is the
251 number of distinct microhaplotypes detected per isolate.

252



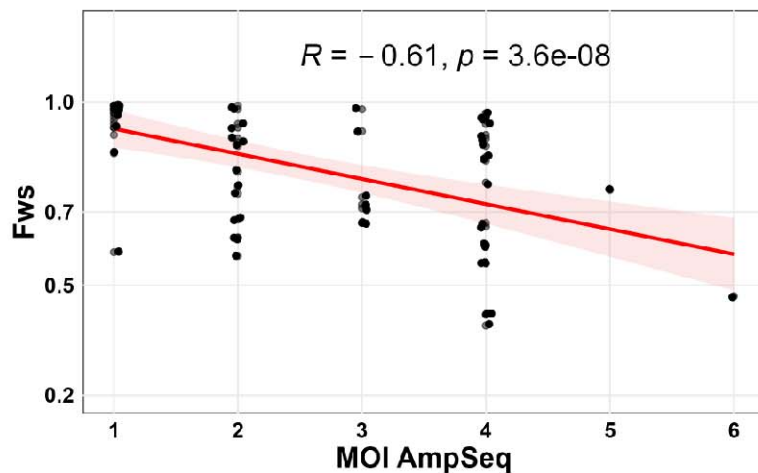
253

254 **Figure 3. Relative proportion of microhaplotypes within patients, from AmpSeq using paired**
255 **gDNA extracted from RBC pellets and plasma samples.** A) Patients with the same
256 microhaplotype profile between plasma and pellet gDNA. B) Patients with more microhaplotypes
257 (higher MOI) detected within RBC pellet gDNA compared to plasma. Each colour indicates a
258 unique microhaplotype within the whole population.

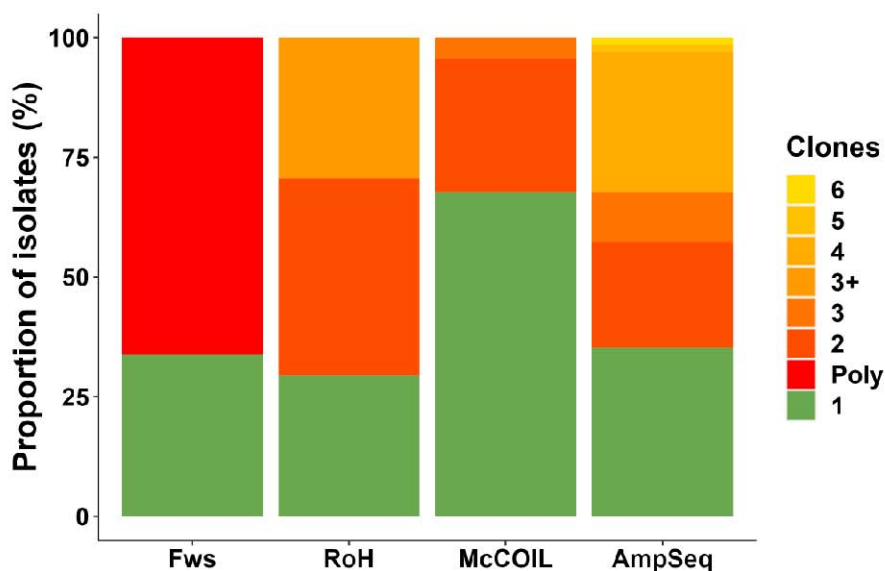
259 **Comparison of AmpSeq and WGS-based methods for determining MOI from pellet gDNA**

260 A total of 68 isolates had MOI data available for both AmpSeq and WGS. We found a good
261 correlation between AmpSeq and the different WGS-based methods ($r = -0.61$, $r = 0.47$ and $r = -0.59$
262 for *Fws*, THE REAL McCOIL and RoH, respectively) (Figure 4). In addition, 80.8% and 79.3% of
263 the isolates showed concordant results (either monoclonal or polyclonal) between AmpSeq and
264 *Fws*, or AmpSeq and RoH, respectively (Figure 4B). However, the AmpSeq method was able to
265 detect up to 6 genotypes in an isolate, indicating greater sensitivity of AmpSeq in detecting multiple
266 genomes in an isolate compared to WGS-based methods (Figure 4B). Furthermore, AmpSeq was
267 the only method capable of quantifying the proportion of each genotype identified within an isolate.
268 Together, these findings showed that the combination of different haplotyping techniques can be
269 used to characterise genetic complexity quantitatively and qualitatively within an isolate. The MOI
270 of a polyclonal isolate was then defined from the AmpSeq data.

A



B



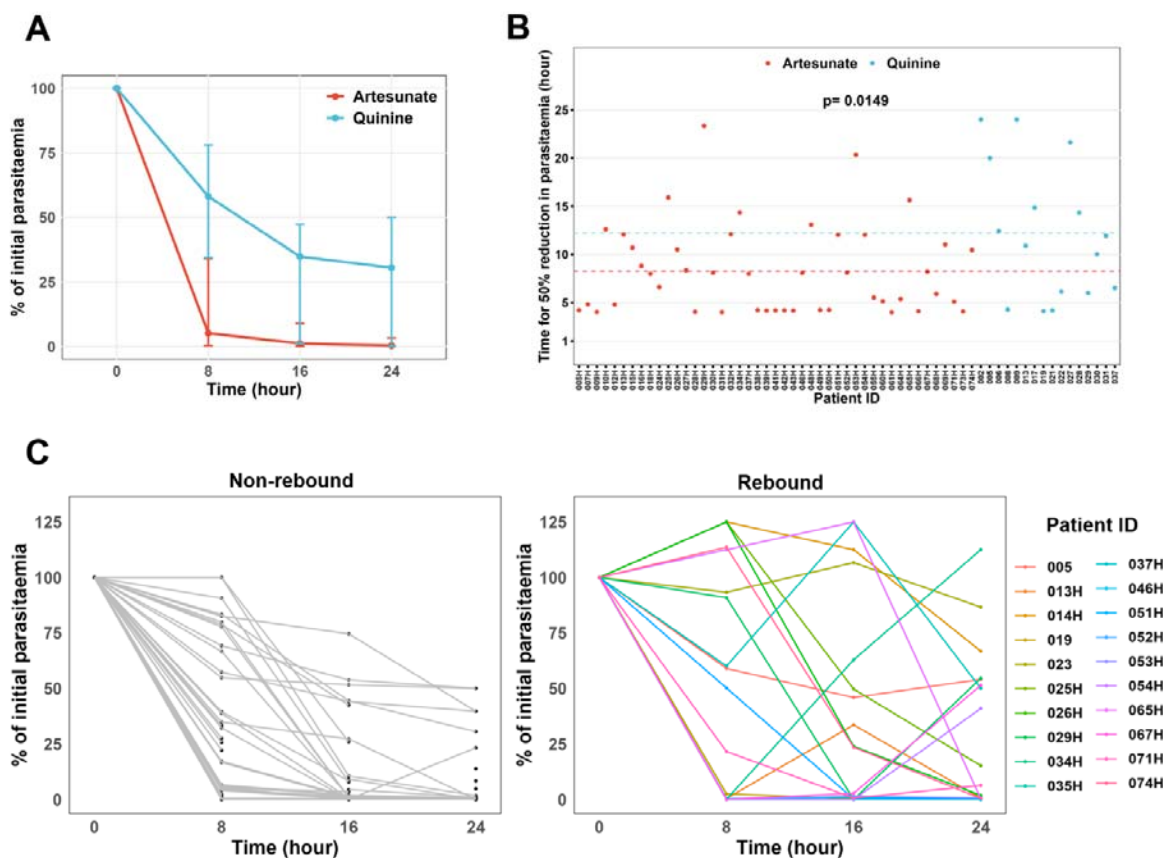
271

272 **Figure 4. Comparison of AmpSeq to different WGS-based algorithms for determining the**
273 **MOI. A) Correlation between *Fws* and AmpSeq. B) Proportion of isolates according to clonality in**
274 **different genotyping techniques. Only individuals with at least one timepoint at *Fws* <0.95 were**
275 **included in this analysis.**

276 **Variability in parasite clearance rate among individuals and high rate of rebound in**
277 **parasitaemia during antimalarial treatment**

278 Having established the most sensitive method for MOI determination, we then aimed to characterise
279 the clearance rate within the first 24 hours of treatment. Median parasite clearance time was faster
280 in children treated with artesunate compared to those treated with quinine (Figure 5A), with the
281 mean PC_{50%} of 8.3 and 12.2 hours, respectively (Figure 5B). There was a high variability in parasite
282 clearance half-life within both treatment groups, ranging from 4.1 to 23.3 hours for artesunate and
283 4.0 to 24.0 hours for quinine (Figure 5B). Of the 48 individuals treated with artesunate, 95.6%
284 (43/45) had a PC_{50%} below 16 hours, compared to 75% (12/16) of individuals treated with quinine
285 (Figure 5B). The PC_{50%} could not be determined for four individuals (023, 014H, 029H, 063H) due
286 to a non-significant decrease in parasitaemia (<50% reduction) between the first and last time points
287 (Supplementary Data 2). Parasite clearance curves are within the same range as previous studies
288 using quinine or artesunate [33] (Supplementary Data 2). These curves indicated substantial
289 variation in initial clearance rates between individuals, highlighting the complex dynamics of
290 parasite response to treatment in the early stage of infection management.

291 We took advantage of the time-series to investigate intra-host competition in polygenomic
292 infections. Interestingly, we observed a ‘rebound’ in the parasitemia determined by microscopy
293 reading. We defined rebound as an increase in parasite densities by at least 100 parasites/μL
294 between two time points, and observed this phenomenon in 34.8% (20/65) of individuals (Figure
295 6C). Specifically, within the artesunate-treated group, 35.4% (17/48) of individuals experienced a
296 rebound, while in the quinine-treated group, the rebound rate was 17.6% (3/17). These data indicate
297 the potential release of sequestered parasites during anti-malarial treatment.



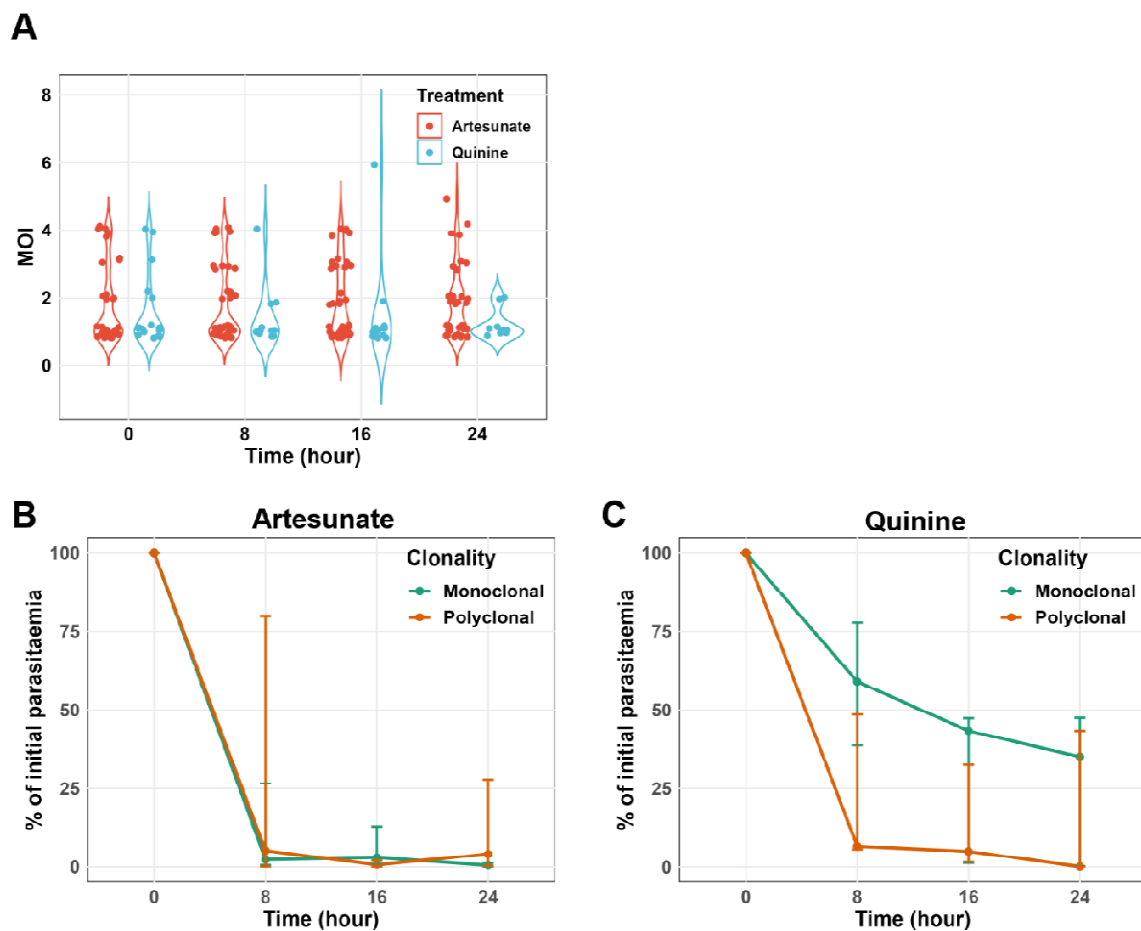
298

299 **Figure 5. Parasite clearance curves of severe malaria cases treated with Artesunate or**
300 **Quinine.** A) Parasite clearance curve according to antimalarial treatment. B) Time for 50%
301 reduction in parasitaemia according to treatment. C) parasite clearance curve highlighting the
302 rebound in parasitaemia post-antimalarial treatment.

303 ***P. falciparum* clearance rate is not related to MOI at the onset of the treatment**

304 To determine whether the variability in the clearance rate of *P. falciparum* depends on the number
305 of parasite genotypes in the infection, the dynamics of parasite clearance were compared between
306 individuals with polyclonal and monoclonal infections during the first 24h of the severe malaria
307 management under treatment pressure. Independently of the treatment administered, the mean MOI
308 was relatively stable throughout the 24-hour period (Figure 6A). In individuals treated with
309 artesunate, *P. falciparum* clearance showed no significant difference between polyclonal and
310 monoclonal infections (Figure 6B). In contrast, although non-significant, treatment with quinine

311 resulted in faster *P. falciparum* clearance in polyclonal infections (mean PC_{50%} of 4.3) compared to
312 monoclonal infections (mean PC_{50%} of 12.4) ($p = 0.1393$) (Figure 6C). Part of this difference may be
313 attributed to the higher median parasitaemia at enrolment in individuals treated with quinine and
314 having monoclonal infections compared to those with polyclonal infections (2440000 vs 1520000
315 p/ μ L, $p = 0.1924$). In addition, there was no correlation between MOI at enrolment and parasite
316 clearance rate ($r = -0.06$, $p = 0.6494$). These data show that the *P. falciparum* clearance rate does not
317 depend on the initial parasite MOI.



318

319 **Figure 6. Dynamic of parasite clearance to parasite multiplicity of the infection.** A) Dynamic of
320 Multiplicity of Infection (MOI) determined by AmpSeq throughout the antimalarial treatment.
321 Parasite clearance rate according to clonality at enrolment (H0) for artesunate (B) quinine (C)
322 treatment groups.

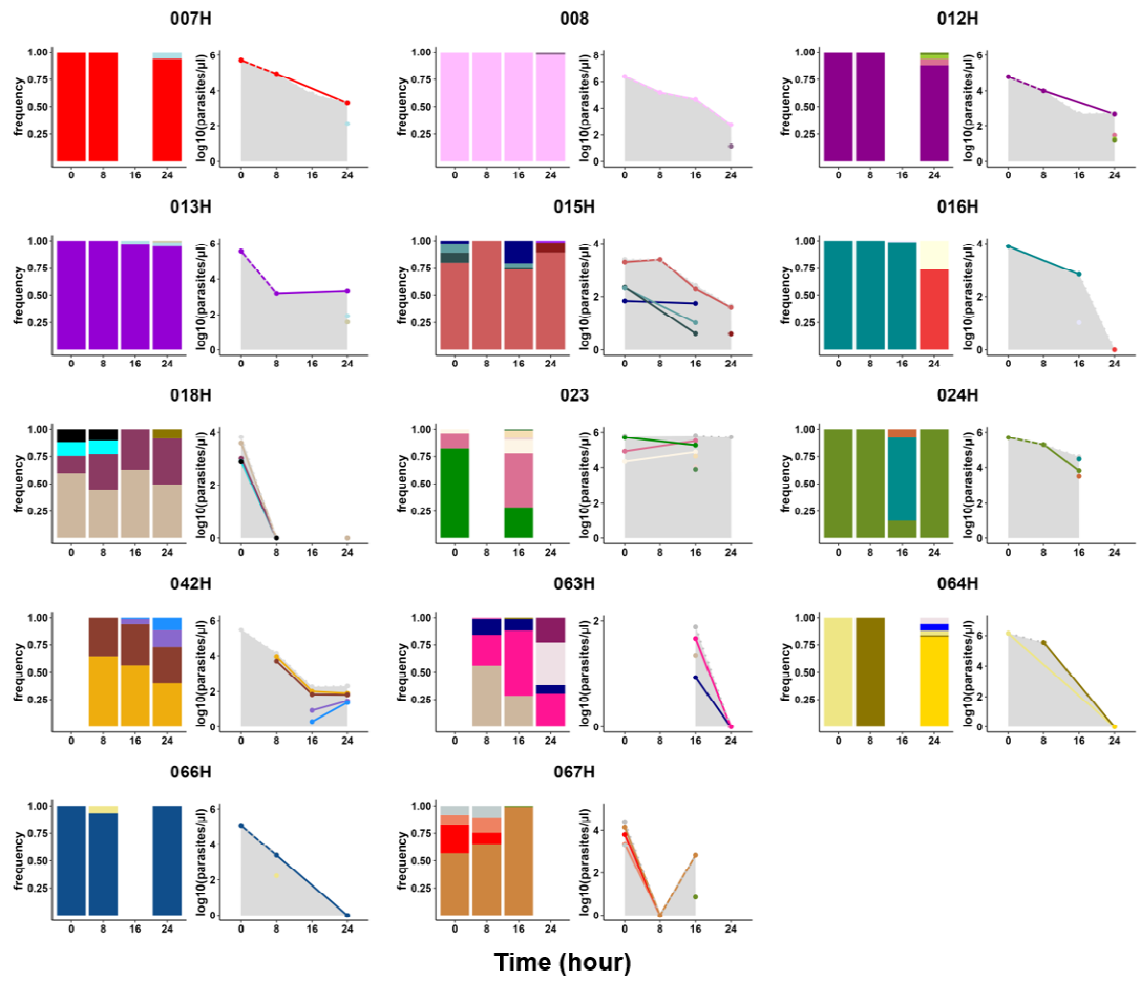
323 **Sporadic detection of novel microhaplotypes during anti-malarial treatment**

324 To measure the complexity of microhaplotypes within each isolate, we measured the Shannon
325 entropy, a metric dependent on the number and proportion of each microhaplotype within an isolate.
326 Despite the overall parasitaemia decreasing by an average of 335-fold over 24 hours, the
327 microhaplotype entropy only slightly decreased between H0 and H8 ($p= 0.0388$), and remained
328 stable afterwards ($p= 0.6093$) (Supplementary Figure 2). This stable MOI is explained by the
329 detection of novel microhaplotypes that were not in circulation at H0. These ‘sporadic’
330 microhaplotypes were detected in over 60.9% (14/23) of participants, predominantly occurring from
331 16 hours after the start of treatment (Figure 7), likely indicating the release of sequestered parasites
332 that were previously undetectable. Additionally, half of participants with sporadic microhaplotypes
333 (007H, 008, 012H, 013H, 016H, 024h, 064H, and 066H) had monoclonal infections at H0 but
334 displayed polyclonal infections at later time points (Figure 7A). However, most of the sporadic
335 microhaplotypes were very minor genotypes (Figure 7A).

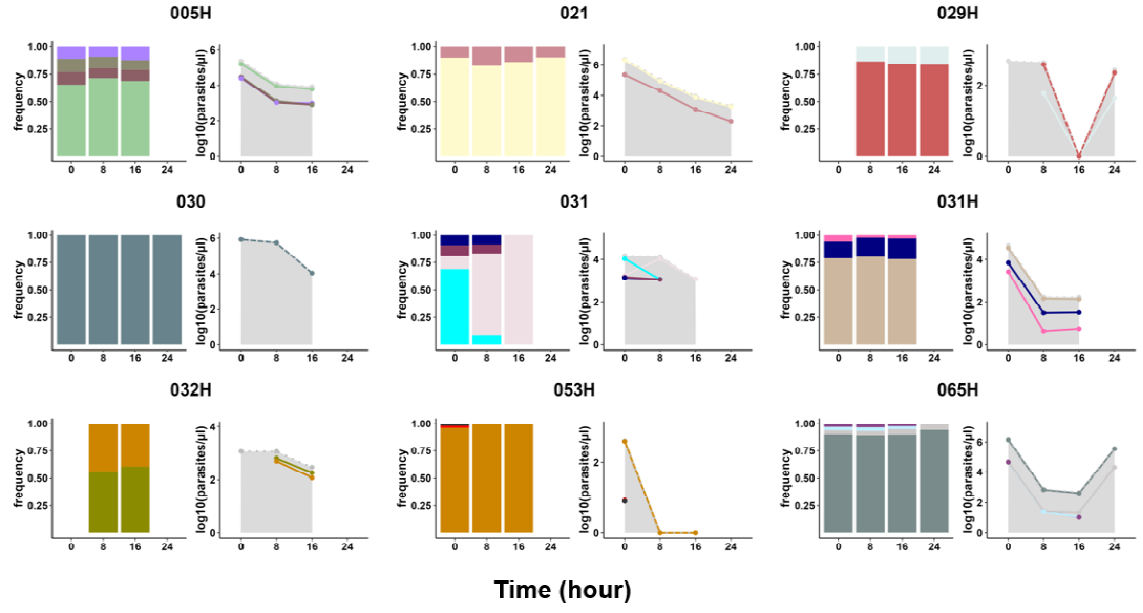
336 We inferred the parasitaemia of each circulating genotype based on the total parasitaemia and the
337 proportion of each microhaplotype. Notably, only one individual (067H) harbouring sporadic
338 microhaplotypes showed a rebound in microhaplotype parasitaemia, indicating that the rebound in
339 total parasitaemia observed was unrelated to the release of new genotypes in circulation after the
340 start of the treatment.

341 Taken together, we here showed that, from blood samples taken on arrival at hospital (H0), it is
342 usually not possible to genotype all *P. falciparum* microhaplotypes from an infection. About two
343 third of the time, one or more distinct strain will appear within 24 hours, presumably as a result of
344 release of sequestered *P. falciparum*.

A



B



346 **Figure 7. Subpopulation clearance curve during anti-malarial treatment, with (A) or without**
347 **(B) sporadic detection of novel microhaplotypes.** The left panel of each plot shows the relative
348 abundance of microhaplotype subpopulations throughout the antimalarial treatment period. The
349 right panel of each plot shows parasite densities of these subpopulations, calculated by multiplying
350 the total parasitaemia by the relative abundance of the microhaplotypes. The clearance curves for
351 the total parasite density are shown as a background surface (in grey). Each color represents a
352 unique microhaplotype within the population. Sporadic detection is defined as the appearance of a
353 new microhaplotype that was not present at H0.

354 **Parasite clearance is not correlated with drug resistance allele frequencies**

355 We tested the hypothesis that drug sensitive genomes get cleared faster, by assessing allelic
356 frequencies of resistance markers *crt*, *mdr1*, *kelch13*, *dhfr* and *dhps* over the 24 hours period. Of the
357 45 individuals for whom baseline drug resistance data was available, 95.6% (43/45) carried
358 chloroquine-resistant allele (K76T) (Supplementary Figure 3A). However, the two individuals
359 showing a mixture of sensitive and resistant alleles came from the group treated with artesunate
360 (Supplementary Figure 3A). The frequency of the multidrug resistance gene 1 (*mdr1*) remained
361 stable in the population throughout the 24 hours treatment period (Supplementary Figure 3B). Only
362 one individual with a k13 mutation (V589I) at the time of enrolment was found in the study
363 population (Supplementary Figure 3C). All isolates carried a triple mutation of the *dhfr* gene (N51I,
364 C59R and S108N) (Supplementary Figure 3D). Similarly, 99% of isolates carried the A437G
365 mutation in the *dhps* gene, with 23.2% and 0% a second mutation (Supplementary Figure 3E).
366 Overall, we observed no alteration in genotypes across all analysed resistance markers within the
367 same individual during antimalarial treatment.

368 Discussion

369 In recent years, several approaches have been used to study the intra-host dynamics of polygenomic
370 infections, including WGS which is the most comprehensive approach for genomic epidemiology,
371 providing a complete picture of genetic variation. However, molecular markers, mainly AmpSeq,
372 which combines several highly polymorphic antigen markers, is now the method of choice for high-
373 resolution detection of MOI [22, 34]. We first aim in this study to evaluate different methods to
374 study intra-host dynamics of polygenomic infections during a course of parasite clearance with an
375 antimalarial treatment. Using the WGS data, we observed a robust correlation between the three
376 algorithms (F_{WS} , THE REAL McCOIL and RoH) used to determine the clonality of an isolate, in
377 particular higher between F_{WS} and RoH with 94.3% consistent results between the two metrics.
378 However, 16.1% of polyclonal isolates according to F_{WS} were classified as monoclonal according to
379 THE REAL McCOIL. These data indicate that both the F_{WS} and RoH algorithms exhibit greater
380 sensitivity in detecting multiple infections compared to THE REAL McCOIL. Indeed, THE REAL
381 McCOIL is a more conservative approach, which provides estimates that minimize overestimation
382 of MOI by considering the likelihood of observed genetic variation being due to multiple parasite
383 strains rather than sequencing errors or technical artefacts [24]. In this study, more than 79% of the
384 isolates showed concordant results (either monoclonal or polyclonal) between AmpSeq and F_{WS} or
385 RoH. However, the AmpSeq method was able to detect up to 6 genotypes in an isolate, indicating
386 greater sensitivity of AmpSeq in detecting multiple genomes in an isolate compared to WGS-based
387 methods. Amplicon sequencing targeting highly polymorphic loci has demonstrated the capability
388 to detect minority haplotypes with frequencies as low as 0.1% [26].

389 Previous studies have demonstrated that plasma can be used to detect and quantify the *Plasmodium*
390 DNA by PCR [20, 21]. However, these studies also indicated that qPCR using whole blood DNA
391 exhibits greater sensitivity than qPCR with plasma DNA. In line with the sequestration
392 phenomenon of *P. falciparum* as shown by quantify the plasma levels of HRP2 or parasite DNA

393 [18, 19], we hypothesized that genotyping parasites using DNA extracted from plasma might detect
394 sequestered *P. falciparum* genotypes. This hypothesis assumes that plasma may contain parasite
395 DNA released from prior schizont ruptures of all the parasite genotypes, which would be unaffected
396 by sequestration at the time of blood sample collection. However, our findings revealed
397 significantly higher microhaplotype complexity in the RBC pellet compared to plasma. These
398 results indicate AmpSeq using gDNA from RBC pellets is more sensitive compared to AmpSeq
399 using gDNA from plasma. To what extent the RBC pellet contains DNA from prior schizont
400 ruptures remains to be determined. Consistent with previous findings where low levels of
401 parasitemia was more effectively detected by qPCR using parasite DNA from whole blood
402 compared to plasma [20], our study also found that parasite load influences the sensitivity of
403 AmpSeq when using plasma as the DNA source. Indeed, the median parasitaemia of isolates with
404 the higher MOI in the RBC pellet compared to plasma was 34.4 fold lower compared to the median
405 parasitaemia of isolates with the same MOI in both biological materials. Interestingly, at
406 parasitaemia levels exceeding 1000 parasites/ μ L, the same multiplicity of infection (MOI) was
407 detected in both plasma and pellet samples in 85.4% of the isolates. This indicates that plasma can
408 be effectively used for parasite genotyping in retrospective studies.

409 We observed high variability in parasite clearance half-life within both treatment groups with faster
410 parasite clearance rate in children treated with artesunate compared to those treated with quinine.
411 Artesunate is a fast-acting antimalarial drug with a pronounced effect on ring-stage parasites,
412 whereas quinine primarily targets mature trophozoites [35]. Rapid clearance results from artesunate
413 action on the circulating ring-stage parasites and their subsequent removal predominantly by the
414 spleen, preventing the parasite sequestration [36, 37]. In line with our findings, a recent study of
415 Ghanaian children showed a prolonged delay in parasite clearance among children with severe
416 malaria, even after three days of treatment with artesunate [38]. This increased time to parasite
417 clearance was associated with age, low haemoglobin levels and high number of previous malaria
418 diagnoses [38]. Other studies have noted variations in parasite clearance rates in children treated for

419 uncomplicated falciparum malaria with artemisinin-based combination therapy, both in Kenya and
420 Tanzania [39, 40]. These findings suggest that factors other than drug resistance may contribute to
421 slower parasite clearance in certain infections, as there is no evidence of artemisinin resistance in
422 these regions. It has been shown that, in areas where artemisinin resistance is not present, the
423 parasite clearance time can be affected by factors such as the age of the host, host acquired
424 immunity, initial parasitemia levels, and the developmental stages of parasite [11–13]. Furthermore,
425 although controversial, studies have shown a link between the genetic complexity of *P. falciparum*
426 and delayed parasite clearance in Africa [14, 15]. Our data show that the *P. falciparum* clearance
427 rate in children with severe malaria independent of parasite MOI at the onset of treatment. Notably,
428 *P. falciparum* clearance was faster in polyclonal infections in quinine-treated children. However,
429 this difference was attributed to significantly higher parasitemia at enrolment in individuals treated
430 with quinine.

431 Interestingly, during antimalarial treatment, a high rate of “rebound” in total parasitemia and
432 specific parasite subpopulations parasitemia was observed. Specifically, an increase in total
433 parasitemia between two time points was detected in 34.8% of individuals. In four individuals (023,
434 031, 063H, and 064H), minor genotypes present at baseline (H0) increased in relative frequency,
435 becoming the dominant microhaplotype. Additionally, sporadic detection of microhaplotypes
436 occurred in over 60.9% of participants, predominantly from 16 hours after treatment initiation. Half
437 of the participants with sporadic microhaplotypes had monoclonal infections at baseline but
438 exhibited polyclonal infections at subsequent time points. These findings potentially highlight
439 release of sequestered *P. falciparum* genotypes during antimalarial treatment [34] Interestingly,
440 none of these sporadic microhaplotypes were detected in pellet or plasma samples at H0, despite the
441 much higher parasite density at that timepoint that would have facilitated detection of a rare
442 genotype. Either these microhaplotypes recently emerged from the liver, with no or little parasite
443 DNA in the plasma yet, or, probably more likely, these sporadic microhaplotypes are present at
444 extremely low parasitaemia making them undetectable in plasma, and were all sequestered at H0.

445 Additionally, a study by Marks et al. (2005) reported a parasitological rebound effect in infants
446 treated with a single dose of sulfadoxine-pyrimethamine, attributed to the selection of drug-resistant
447 parasites shortly after drug clearance [41]. However, no mutation associated with artemisinin
448 resistance has yet been identified in Benin [9, 10]. In addition, no alterations were observed in allele
449 frequencies across all analysed resistance markers within the same individual post-antimalarial
450 treatment. Two other studies using AmpSeq detected sporadic microhaplotypes or an increase in the
451 frequency of minor microhaplotypes during the treatment of uncomplicated *P. falciparum* infections
452 in regions with no signs of artemisinin resistance [39, 40]. In *falciparum* malaria, parasitized red
453 blood cells circulate in the peripheral blood for only one-third of the 48-hour asexual cycle [42]; for
454 the remainder of the cycle, they are sequestered in the venules and capillaries. For these infections,
455 the peripheral blood parasitemia at a given time point does not reflect the total parasite burden.

456 Limitations of this study include the lack of sampling timepoints beyond 24 hours post-treatment,
457 which affected the accurate determination of parasite clearance half-life for some individuals using
458 the standard WWARN method [43]. This was due to the fact that the parasitemia reduction rate was
459 less than 50% of the initial parasitemia at the last recorded timepoint. Therefore, we used linear
460 interpolation to estimate the time required for a 50% reduction in parasitaemia, referred as the
461 extrapolated parasite clearance half-life (PC_{50%}). However, unlike therapeutic efficacy studies
462 typically focusing on day 3, 7 and 21/28, we were able to monitor the dynamics of *P. falciparum*
463 complexity during the initial management of severe malaria.

464 This study demonstrates that combining different haplotyping techniques can effectively determine
465 genetic complexity. However, AmpSeq is the most sensitive approach and should be the first choice
466 for genotyping to monitor the evolution of genotype clearance following antimalarial treatment.
467 Additionally, plasma can be effectively used for parasite genotyping at sufficient parasitaemia
468 levels. We demonstrated that genotyping a blood sample from a patient on arrival at hospital is
469 typically not sufficient to detect all parasites genotypes present in the infection.

470 **Conflicts of interest**

471 No conflicts of interest were reported by the authors.

472 **Financial support**

473 This work was funded by grants from the French National Research Agency
474 (18CE15000901), the ATIP-Avenir programme and by Institut Merieux. The “SPF Post doc
475 en France” programme of the “Fondation pour la Recherche Médicale” funded the author “Balotin
476 Fogang” (SPF202209015889).

477 **Ethical approval**

478 Ethical clearance was obtained from “Comité d’Ethique de la Recherche CER_ISBA Benin”
479 (clearance n°90, 06/06/2016 and clearance n°38, 16/05/2014).

480 **Acknowledgments**

481 We would like to thank the participants and their parents/guardians for granting approval to
482 participate in this study. We thank the staff of the paediatric wards at the CHUMEL hospital in
483 Cotonou and at Saint Joseph medical centre in Sô-Tchanhoué, Benin, for their help. Our thanks go
484 to MalariaGen for the whole genome sequencing and to the GenSeq platform for the amplicon
485 sequencing.

486 **Author contributions**

487 Conceptualization by A.C and G.I.B. Field work and sample processing by C.K, S.E and G.A. Data
488 analysis by B.F, E.G. Writing of original draft by B.F, E.G. Reviewing and editing of manuscript by
489 B.F., E.G, C.K, G.I.B, A.C. Funding acquisition by A.C and G.I. B.

490 **Data availability**

491 All whole-genome sequencing (WGS) data generated and analyzed in this study have been
492 deposited in the European Nucleotide Archive (ENA) under the study accession number
493 PRJEB2136, with individual accession numbers in Supplementary Table 1. The raw reads from the
494 Amplicon sequencing (AmpSeq) data are publicly available on Zenodo
495 (<https://zenodo.org/records/13224728>), with corresponding individual accession numbers provided
496 in Supplementary Table 3. The raw data and complete AmpSeq results are included as
497 Supplementary Tables 1 and 2, respectively.

498 **Description of supplementary Material**

499 **Supplementary Figure 1. Parasitaemia according to the concordance between MOI from**
500 **paired RBC pellet and plasma samples, determined by AmpSeq.** "Pellet-plasma match" are
501 isolates with identical MOI in plasma and pellet samples. "Low in plasma" are isolates in which the
502 measured MOI was lower in plasma compared to pellet samples. There were only 2 isolates with
503 MOI higher in the plasma than in the pellet, which are not shown on this figure.

504 **Supplementary Figure 2. Microhaplotype entropy over time during antimalarial treatment.**

505 **Supplementary Figure 3. Frequency of antimalarial drug resistance markers throughout**
506 **treatment.**

507 **Supplementary Table 1. Epidemiological data of study participants.**

508 **Supplementary Table 2. PCR primers sequences and amplification conditions.** List of forward
509 and reverse primers used for AmpSeq and the amplification program.

510 **Supplementary Table 3. Amplicon Sequencing results.** AmpSeq read counts and frequencies, for
511 three markers (*cpmp*, *ama1-D3*, *cpp*) used in both plasma and red blood cell pellets. The table
512 identifies the selected marker for each individual, with the marker displaying the highest number of
513 microhaplotypes being retained. The last column indicates 'sporadic' microhaplotypes, defined as
514 novel microhaplotypes not detected at H0.

515 **Appendix 1. Determining the Multiplicity of Infection (MOI) based on Whole Genome**
516 **Sequencing (WGS).**

517 **Supplementary Data 1. Non-reference allele frequency (NRAF) distribution across all**
518 **heterozygous SNPs (left) and heterozygosity calculated in 100-kb bins (right) to highlight**
519 **RoH.**

520 **Supplementary Data 2. Individuals parasite clearance curve by timepoints post-antimalarial**
521 **treatment. Quinine (A) and artesunate (B) treated groups.**

522 **References**

- 523 1. **White NJ.** Severe malaria. *Malar J* 2022;21:284.
- 524 2. **WHO.** *Management of severe malaria: a practical handbook*. 3rd ed. Geneva: World Health
525 Organization. <https://iris.who.int/handle/10665/79317> (2012, accessed 18 June 2024).

- 526 3. **Dondorp AM, Fanello CI, Hendriksen IC, Gomes E, Seni A, et al.** Artesunate versus quinine
527 in the treatment of severe falciparum malaria in African children (AQUAMAT): an open-label,
528 randomised trial. *Lancet* 2010;376:1647–1657.
- 529 4. **Phyo AP, Nosten F, Phyo AP, Nosten F.** The Artemisinin Resistance in Southeast Asia: An
530 Imminent Global Threat to Malaria Elimination. In: *Towards Malaria Elimination - A Leap*
531 *Forward*. IntechOpen. Epub ahead of print 18 July 2018. DOI: 10.5772/intechopen.76519.
- 532 5. **Pluijm RW van der, Imwong M, Chau NH, Hoa NT, Thuy-Nhien NT, et al.** Determinants
533 of dihydroartemisinin-piperaquine treatment failure in Plasmodium falciparum malaria in
534 Cambodia, Thailand, and Vietnam: a prospective clinical, pharmacological, and genetic study.
535 *Lancet Infect Dis* 2019;19:952–961.
- 536 6. **Assefa A, Fola AA, Tasew G.** Emergence of Plasmodium falciparum strains with artemisinin
537 partial resistance in East Africa and the Horn of Africa: is there a need to panic? *Malar J*
538 2024;23:34.
- 539 7. **Balikagala B, Fukuda N, Ikeda M, Katuro OT, Tachibana S-I, et al.** Evidence of
540 Artemisinin-Resistant Malaria in Africa. *N Engl J Med* 2021;385:1163–1171.
- 541 8. **Ariey F, Witkowski B, Amaratunga C, Beghain J, Langlois A-C, et al.** A molecular marker
542 of artemisinin-resistant Plasmodium falciparum malaria. *Nature* 2014;505:50–55.
- 543 9. **Kpemasse A, Dagnon F, Saliou R, Yarou Maye AS, Affoukou CD, et al.** Efficacy of
544 Artemether-Lumefantrine for the Treatment of Plasmodium falciparum Malaria in Bohicon and
545 Kandi, Republic of Benin, 2018–2019. *Am J Trop Med Hyg* 2021;105:670–676.
- 546 10. **L’Episcopia M, Doderer-Lang C, Perrotti E, Priuli GB, Cavallari S, et al.** Polymorphism
547 analysis of drug resistance markers in Plasmodium falciparum isolates from Benin. *Acta Trop*
548 2023;245:106975.

- 549 11. **Ataide R, Ashley EA, Powell R, Chan J-A, Malloy MJ, et al.** Host immunity to Plasmodium
550 falciparum and the assessment of emerging artemisinin resistance in a multinational cohort.
551 *Proc Natl Acad Sci U S A* 2017;114:3515–3520.
- 552 12. **Intharabut B, Kingston HW, Srinamon K, Ashley EA, Imwong M, et al.** Artemisinin
553 Resistance and Stage Dependency of Parasite Clearance in Falciparum Malaria. *J Infect Dis*
554 2019;219:1483–1489.
- 555 13. **WWARN Parasite Clearance Study Group, Abdulla S, Ashley EA, Bassat Q, Bethell D, et**
556 *al.* Baseline data of parasite clearance in patients with falciparum malaria treated with an
557 artemisinin derivative: an individual patient data meta-analysis. *Malar J* 2015;14:359.
- 558 14. **Kyabayinze DJ, Karamagi C, Kiggundu M, Kanya MR, Wabwire-Mangen F, et al.**
559 Multiplicity of Plasmodium falciparum infection predicts antimalarial treatment outcome in
560 Ugandan children. *Afr Health Sci* 2008;8:200–205.
- 561 15. **Topazian HM, Moser KA, Ngasala B, Oluoch PO, Forconi CS, et al.** Low Complexity of
562 Infection Is Associated With Molecular Persistence of Plasmodium falciparum in Kenya and
563 Tanzania. *Front Epidemiol*;2. Epub ahead of print 6 June 2022. DOI:
564 10.3389/fepid.2022.852237.
- 565 16. **Cunnington AJ, Bretscher MT, Nogaro SI, Riley EM, Walther M.** Comparison of parasite
566 sequestration in uncomplicated and severe childhood Plasmodium falciparum malaria. *J Infect*
567 2013;67:220–230.
- 568 17. **Dondorp AM, Desakorn V, Pongtavornpinyo W, Sahassananda D, Silamut K, et al.**
569 Estimation of the total parasite biomass in acute falciparum malaria from plasma PfHRP2. *PLoS*
570 *Med* 2005;2:e204.

- 571 18. **Fukuda N, Balikagala B, Ueno T, Anywar DA, Kimura E, et al.** The Impact of Sequestration
572 on Artemisinin-Induced Parasite Clearance in Plasmodium falciparum Malaria in Africa. *Clin*
573 *Infect Dis Off Publ Infect Dis Soc Am* 2023;76:1585–1593.
- 574 19. **Imwong M, Stepniewska K, Tripura R, Peto TJ, Lwin KM, et al.** The numerical
575 distributions of parasite densities in asymptomatic malaria. *J Infect Dis*.
- 576 20. **Lamikanra AA, Dobaño C, Jiménez A, Nhabomba A, Tsang HP, et al.** A direct comparison
577 of real time PCR on plasma and blood to detect Plasmodium falciparum infection in children.
578 *Malar J* 2012;11:201.
- 579 21. **Sambe BS, Diagne A, Diatta HAM, Gaba FM, Sarr I, et al.** Molecular detection and
580 quantification of Plasmodium vivax DNA in blood pellet and plasma samples from patients in
581 Senegal. *Front Parasitol*;2. Epub ahead of print 24 April 2023. DOI:
582 10.3389/fpara.2023.1149738.
- 583 22. **Ruybal-Pesántez S, McCann K, Vibin J, Siegel S, Auburn S, et al.** Molecular markers for
584 malaria genetic epidemiology: progress and pitfalls. *Trends Parasitol* 2024;40:147–163.
- 585 23. **Manske M, Miotto O, Campino S, Auburn S, Almagro-Garcia J, et al.** Analysis of
586 Plasmodium falciparum diversity in natural infections by deep sequencing - Nature. *Nature*
587 2012;487:375–379.
- 588 24. **Chang H-H, Worby CJ, Yeka A, Nankabirwa J, Kamya MR, et al.** THE REAL McCOIL: A
589 method for the concurrent estimation of the complexity of infection and SNP allele frequency
590 for malaria parasites. *PLoS Comput Biol* 2017;13:e1005348.
- 591 25. **Pearson RD, Amato R, Auburn S, Miotto O, Almagro-Garcia J, et al.** Genomic analysis of
592 local variation and recent evolution in Plasmodium vivax. *Nat Genet* 2016;48:959–964.

- 593 26. **Lerch A, Koepfli C, Hofmann NE, Messerli C, Wilcox S, et al.** Development of amplicon
594 deep sequencing markers and data analysis pipeline for genotyping multi-clonal malaria
595 infections. *BMC Genomics* 2017;18:864.
- 596 27. **Kamaliddin C, Rombaut D, Guillochon E, Royo J, Ezinmegnon S, et al.** From genomic to
597 LC-MS/MS evidence: Analysis of PfEMP1 in Benin malaria cases. *PLOS ONE*
598 2019;14:e0218012.
- 599 28. **MalariaGEN, Ahouidi A, Ali M, Almagro-Garcia J, Amambua-Ngwa A, et al.** An open
600 dataset of Plasmodium falciparum genome variation in 7,000 worldwide samples. *Wellcome*
601 *Open Res* 2021;6:42.
- 602 29. **Danecek P, Bonfield JK, Liddle J, Marshall J, Ohan V, et al.** Twelve years of SAMtools and
603 BCFtools. *GigaScience* 2021;10:giab008.
- 604 30. **Quinlan AR, Hall IM.** BEDTools: a flexible suite of utilities for comparing genomic features.
605 *Bioinforma Oxf Engl* 2010;26:841–842.
- 606 31. **Gruenberg M, Lerch A, Beck H-P, Felger I.** Amplicon deep sequencing improves
607 Plasmodium falciparum genotyping in clinical trials of antimalarial drugs. *Sci Rep*
608 2019;9:17790.
- 609 32. **R Core Team.** R: A Language and Environment for Statistical Computing.
- 610 33. **White NJ.** Malaria parasite clearance. *Malar J* 2017;16:88.
- 611 34. **Jones S, Kay K, Hodel EM, Gruenberg M, Lerch A, et al.** Should Deep-Sequenced
612 Amplicons Become the New Gold Standard for Analyzing Malaria Drug Clinical Trials?
613 *Antimicrob Agents Chemother*;65. Epub ahead of print October 2021. DOI:
614 10.1128/AAC.00437-21.

- 615 35. **Wilson DW, Langer C, Goodman CD, McFadden GI, Beeson JG.** Defining the Timing of
616 Action of Antimalarial Drugs against *Plasmodium falciparum*. *Antimicrob Agents Chemother*
617 2013;57:1455–1467.
- 618 36. **Chotivanich K, Udomsangpetch R, McGready R, Proux S, Newton P, et al.** Central role of
619 the spleen in malaria parasite clearance. *J Infect Dis* 2002;185:1538–1541.
- 620 37. **Udomsangpetch R, Pipitaporn B, Krishna S, Angus B, Pukrittayakamee S, et al.**
621 Antimalarial drugs reduce cytoadherence and rosetting *Plasmodium falciparum*. *J Infect Dis*
622 1996;173:691–698.
- 623 38. **Paris L, Tackie RG, Beshir KB, Tampuori J, Awandare GA, et al.** Parasite clearance
624 dynamics in children hospitalised with severe malaria in the Ho Teaching Hospital, Volta
625 Region, Ghana. *Parasite Epidemiol Control* 2022;19:e00276.
- 626 39. **Mideo N, Bailey JA, Hathaway NJ, Ngasala B, Saunders DL, et al.** A deep sequencing tool
627 for partitioning clearance rates following antimalarial treatment in polyclonal infections. *Evol*
628 *Med Public Health* 2016;2016:21–36.
- 629 40. **Wamae K, Kimenyi KM, Osofi V, Laurent ZR de, Ndwiga L, et al.** Amplicon Sequencing as
630 a Potential Surveillance Tool for Complexity of Infection and Drug Resistance Markers in
631 *Plasmodium falciparum* Asymptomatic Infections. *J Infect Dis* 2022;226:920.
- 632 41. **Marks F, von Kalckreuth V, Kobbe R, Adjei S, Adjei O, et al.** Parasitological rebound effect
633 and emergence of pyrimethamine resistance in *Plasmodium falciparum* after single-dose
634 sulfadoxine-pyrimethamine. *J Infect Dis* 2005;192:1962–1965.
- 635 42. **White NJ.** The parasite clearance curve. *Malar J* 2011;10:278.
- 636 43. **Flegg JA, Guerin PJ, White NJ, Stepniwska K.** Standardizing the measurement of parasite
637 clearance in *falciparum* malaria: the parasite clearance estimator. *Malar J* 2011;10:339.